

# Self-diffusiophoresis of Janus particles in near-critical mixtures

Alois Würger

Laboratoire Ondes et Matière d'Aquitaine, Université de Bordeaux & CNRS,  
351 cours de la Libération, 33405 Talence, France

We theoretically study the self-propulsion of a laser-heated Janus particle in a near critical water-lutidine mixture, and relate its velocity  $v_p$  and squirmer parameter  $\beta$  to the wetting properties of its two hemispheres. For non-ionic surface forces, the particle moves the active cap at the front, whereas a charged hydrophilic cap leads to backward motion, in agreement with experiment. Both  $v_p$  and  $\beta$  show non-monotonic dependencies on the heating power, and may even change sign. The variation of  $\beta$  is expected to strongly affect the collective behavior of dense squirmer systems.

PACS numbers 05.70.Ln; 66.10.C-; 82.70.-Dd

PACS numbers:

In recent years, artificial microswimmers have been realized by Janus particles which move along the concentration or temperature gradients generated by their own chemical or thermal activity [1–5]. Oriented autonomous motion has been achieved through dynamical feedback [6] or rectification in a periodically structured channel [7], opening applications such as targeted transport and pumping of passive particles. In dense systems, active Janus particles aggregate in dynamical clusters [8, 9]. This observation was related to short-range hydrodynamic effects [10–12], in terms of the squirmer model originally developed for the motility of bacteria. Self-propulsion mechanisms have generally a strong diffusiophoretic component [13, 14]; in the case of ionic molecular solutes, self-generated electric fields and ion effects may contribute to the motion [15, 16].

Diffusiophoresis was first rationalized by Derjaguin et al. [17], when observing that wax particles dispersed in a non-uniform glucose solution, migrate toward lower sugar concentration. Because of its unfavorable interaction with wax ( $u > 0$ ), sugar is depleted in the boundary layer, the adsorption parameter  $\Gamma = \int_0^\infty dz z (e^{-u/k_B T} - 1)$  is negative, and the wax particle migrates to lower glucose content at the velocity [18]

$$v_p = \frac{2k_B T}{3\eta} \Gamma \nabla n, \quad (1)$$

where  $\eta$  is the solvent viscosity. For a molecular solute that is attracted by the surface, one has  $\Gamma > 0$  and the particle moves toward higher concentration.

There is no such simple rule for self-propelling Janus particles, where both the adsorption parameter and the concentration gradient vary along the particle surface, and where catalytic coating may result in a multicomponent boundary layer [13, 19]. A particularly intricate situation occurs for hot Janus particles in a near-critical water-lutidine mixture [4], which migrate in a self-generated composition gradient. Though their motion is clearly related to the wetting properties of their active and passive surfaces [9, 20], there is at present no explanation for the sign and magnitude of the velocity.

In this Letter we study self-diffusiophoresis in such near-critical binary mixtures [4, 9, 20]. Starting from

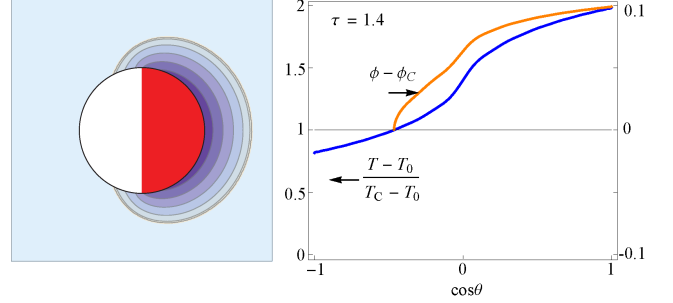


FIG. 1: Critical droplet ( $\phi > \phi_C$ ) surrounding a particle with hydrophilic surface coating on both the cap (red) and the uncapped hemisphere (white). The surface temperature profile  $T(\mathbf{r})$  (calculated from the thin-cap limit of Ref. [21]) and the composition (from (2) with  $C = 100^\circ\text{C}$ ) are plotted as a function of the cosine of the polar angle. The scale of the reduced temperature  $(T - T_0)/(T_C - T_0)$  is on the left ordinate, and that of the water content  $\phi - \phi_C$  on the right one. The parameter  $\tau = (T_m - T_0)/(T_C - T_0)$  depends on the temperature at midplane  $T_m$ .

the properties of the demixing volume surrounding the particle, we evaluate the velocity  $v_p$  and the squirmer parameter  $\beta$ , both of which depend in an intricate manner on the heating power and the dispersion forces exerted by the two hemispheres. Finally, we compare with recent experiments and discuss charge effects.

*The critical droplet.* Fig. 1 illustrates an active Janus particle in a water-lutidine mixture at the critical water content  $\phi_C = 0.72$  and at a bulk temperature  $T_0$  which is slightly below the critical value  $T_C = 34.1^\circ\text{C}$ . Illuminating the particle with a laser beam, results in a temperature profile  $T(\mathbf{r})$  that exceeds  $T_C$  on part or all of the surface, and thus causes local demixing. Assuming a quadratic relation to the local composition,  $T - T_C = C(\phi - \phi_C)^2$ , one finds the change of water content

$$\phi(\mathbf{r}) - \phi_C = \pm \sqrt{\frac{T(\mathbf{r}) - T_C}{C}}, \quad (2)$$

where the two signs correspond to water-rich and lutidine-rich phases, and where  $C \sim 100^\circ\text{C}$  [22]. This

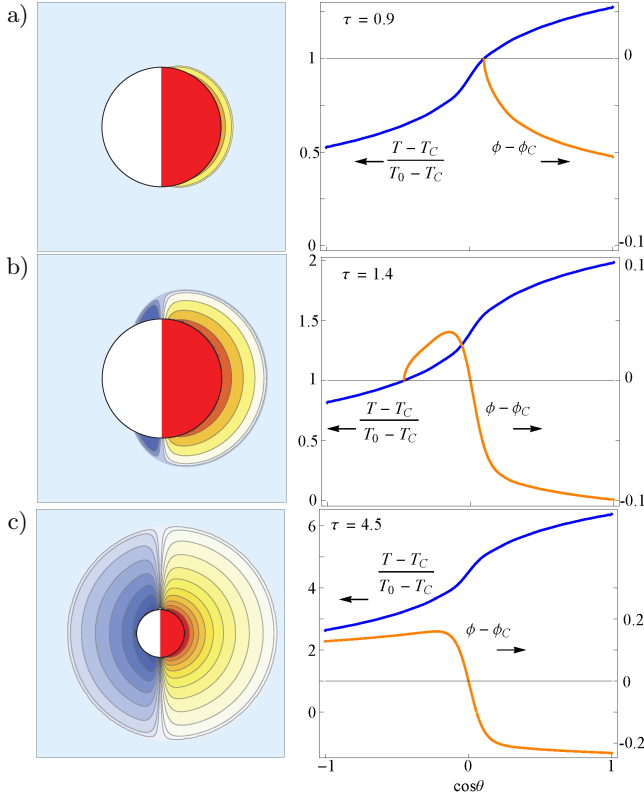


FIG. 2: Demixing volume surrounding a particle with hydrophobic cap and hydrophilic remainder. Heating power increases from a) to c); the right panels show temperature and composition profiles as in Fig. 1. a) The critical condition is satisfied only in a thin lutidine-rich droplet that partly covers the cap. b) Most of the surface is above  $T_C$ ; the cap is surrounded by the lutidine-rich phase, and the hydrophilic remainder by the water-rich phase. The phase boundary is modelled by a factor  $\tanh(\cos \theta/c_0)$  with  $c_0 = 0.1$ . c) Strong heating leads to  $T > T_C$  on the entire surface and to a spherical demixing volume.

mean-field relation ceases to be valid at the critical point where composition fluctuations become long-range.

A more complex situation occurs for a particle with a hydrophobic cap, as illustrated in Fig. 2. If  $T_C$  is reached on both hemispheres, the critical volume splits in lutidine-rich and water-rich compartments, with the phase boundary attached at the particle's midplane [23]. This separation is possible since the interface tension between the spinodal phases,  $\gamma < 10^{-4}$  N/m for  $T < 36$  °C [22], is much smaller than the particle's surface energy. For the strong-heating case (c), the critical volume is almost spherical, and its radius  $\tau a$  much larger than that of the particle,  $a$ . Experiments cover the whole range of tens of microns [20].

*Slip velocity.* Contrary to the demixing volume, the boundary layer is not in a quiescent state, but shows a non-uniform pressure and a steady diffusion current. Assuming that mutual diffusion of water-lutidine is faster than advection and inserting the current in Stokes' equa-

tion, one finds the effective slip velocity [24],

$$v_s = -\frac{k_B T}{\bar{v} \eta} \Gamma \frac{d\phi}{dx}, \quad (3)$$

where we have defined the mean inverse molecular volume  $\bar{v}^{-1} = \phi_C v_l^{-1} + (1 - \phi_C) v_w^{-1}$  and the adsorption parameter

$$\Gamma = \int_0^\infty dz z \frac{e^{-\psi_w} - e^{-\psi_l}}{\phi e^{-\psi_w} + (1 - \phi) e^{-\psi_l}}. \quad (4)$$

The effective potential of water and lutidine,  $\psi_w$  and  $\psi_l$  are given in units of the thermal energy, and vanish well beyond the interaction range  $\lambda$ . In the dilute limit  $\phi \rightarrow 0$  and with  $u = k_B T(\psi_w - \psi_l)$ , one recovers Derjaguin's adsorption factor in (1). Note that the slip velocity  $v_s$  does not depend on the parallel force component  $\partial_x \psi$ , but on the composition gradient only [28].

For an order-of-magnitude estimate, it is convenient to explicit the adsorption parameter for a square well potential of width  $\lambda$  and prefactor  $\bar{\psi}$ , where the integral in (4) gives  $\frac{1}{2} \lambda^2$  with  $\psi_i \rightarrow \bar{\psi}_i$  in the second factor. A strongly hydrophobic surface repels water and attracts lutidine ( $\bar{\psi}_w > \bar{\psi}_l$ ), such that  $\Gamma < 0$ , whereas a hydrophilic surface is characterized by  $\Gamma > 0$ . With typical parameters [20] we find  $\Gamma \sim 10^{-21}$  m<sup>2</sup> and, supposing an interaction length  $\lambda$  of a few Å, we deduce  $\bar{\psi}_i \sim 10^{-2}$ . Then the adsorption parameter  $\Gamma = \frac{1}{2} \lambda^2 (\bar{\psi}_l - \bar{\psi}_w)$  takes a constant value  $\Gamma_{\text{cap}}$  on the cap, and  $\Gamma_{\text{unc}}$  on the remainder.

*Self-propulsion.* The particle velocity is obtained by averaging the slip velocity over the surface,  $\mathbf{v}_p = -\langle \mathbf{v}_s \rangle$  [29]. For an axisymmetric particle one finds

$$v_p = \frac{k_B T}{2 \bar{v} \eta a} \int_{-1}^1 dc (1 - c^2) \Gamma \partial_c \phi, \quad (5)$$

where we have used the relation  $\partial_x = a^{-1} \sqrt{1 - c^2} \partial_c$  between the local coordinate  $x$  and the cosine of the polar angle  $c = \cos \theta$ . Sign and magnitude of the velocity are determined by the product of the adsorption factor  $\Gamma$  and the derivative of the composition gradient  $\partial_c \phi$ . A particularly complex behavior occurs for cases as in Fig. 2, where  $\Gamma_{\text{cap}}$  and  $\Gamma_{\text{unc}}$  take opposite signs and where the gradient  $\partial_c \phi$  is largest in the midplane area.

In Fig. 3 we plot the particle velocity as a function of the surface temperature at midplane  $T_m$ , in terms of the reduced quantity  $\tau = (T_m - T_0)/(T_C - T_0)$ . Critical conditions on the summit of the cap are reached at  $\tau_C = 1/\sqrt{2}$ , on the particle's midplane at  $\tau_m = 1$ , and on the entire surface at  $\tau_S = 1 + 1/\sqrt{2}$ . The behavior of the velocity is to a large extent determined by the ratio of adsorption parameters  $\xi = \Gamma_{\text{unc}}/\Gamma_{\text{cap}}$ ; that is, by the wetting properties of the two hemispheres. We distinguish three parameter ranges.

(i) For  $\tau_C < \tau < 1$ , the critical droplet covers only part of the cap, as in Fig. 2a. Since in this range,  $\Gamma$  and  $\partial_c \phi$  carry the same sign, the particle moves forward ( $v_p > 0$ ) for both hydrophobic and hydrophilic coating. The velocity is independent of  $\Gamma_{\text{unc}}$ .

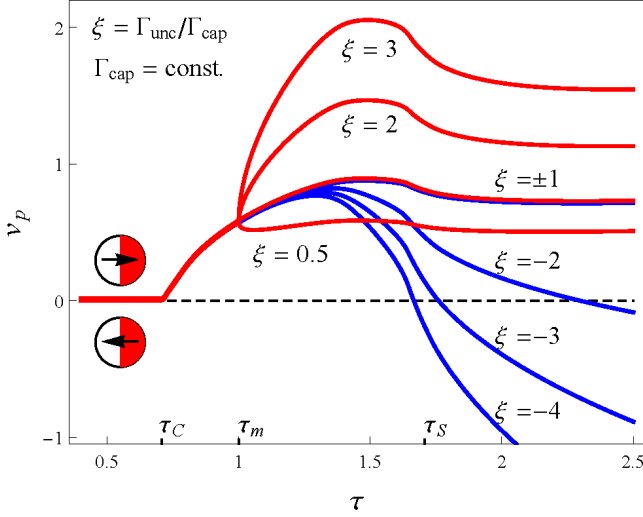


FIG. 3: Self-propulsion velocity  $v_P$  as a function of  $\tau = (T_m - T_0)/(T_C - T_0)$ , for different values of adsorption parameters. Positive  $v_P$  means that the particle moves forward (cap at the front). We fix the adsorption parameter of the cap and vary the ratio  $\xi = \Gamma_{\text{unc}}/\Gamma_{\text{cap}}$ . Self-propulsion sets in at  $\tau_C = 1/\sqrt{2}$ . If the critical droplet extends to both hemispheres ( $\tau > 1$ ), the velocity strongly depends on  $\xi$  and changes sign for  $\xi < -1$ . The velocity scale is of the order of  $\mu\text{m/s}$ .

(ii) In the range  $1 < \tau$  and  $\xi > 0$ , both hemispheres contribute to the integral in (5). The cusp at  $\tau_m$  occurs because of the large derivative  $\partial_c \phi$  on the uncapped hemisphere; see the right panel of Fig. 1. The velocity goes through a maximum at  $\tau \approx 1.5$ , where most of the particle is covered by the critical volume; at strong driving  $\tau \gg 1$ , it increases as  $v_P \propto (1 + \xi)\sqrt{\tau}$  [24].

(iii) For  $1 < \tau$  and  $\xi < 0$ , the velocity is to a large extent determined by the change of sign of  $\phi - \phi_C$  at mid-plane, where the contributions of the two hemispheres partly cancel in (5). If the adsorption parameter is larger on the uncapped part,  $\xi < -1$ , it dominates the velocity and finally results in a change of sign; well beyond  $\tau_S$  one finds  $v_P \propto (1 - \xi)\sqrt{\tau}$  [24].

Several features can be traced back to the relation between the laser intensity  $I$  and the excess temperature. With  $T_m - T_0 = I\chi a/2\kappa$ , the heat conductivity  $\kappa$ , and the absorption coefficient per unit area  $\chi$ , one finds

$$v_P \propto \frac{f(I - I_C)}{\sqrt{a}}, \quad I_C = \frac{\sqrt{2}\kappa}{\chi a} (T_C - T_0). \quad (6)$$

In a very narrow range above  $\tau_C$  one has  $f(x) = x^{3/2}$  (invisible in Fig. 3); the cusp at  $\tau_m$  follows the law  $\sqrt{I - I_m}$ .

We briefly discuss the above result in view of recent experiments. At small or moderate driving we expect the particles to move the cap at the front. This agrees with observations on carbon-capped silica beads [9] and gold-capped particles with hydrophobic coating [20]. In addition, the size dependencies of (6) and the overall shape of  $v_P$  agree well with the data of Buttini et al. (Fig. 4a of

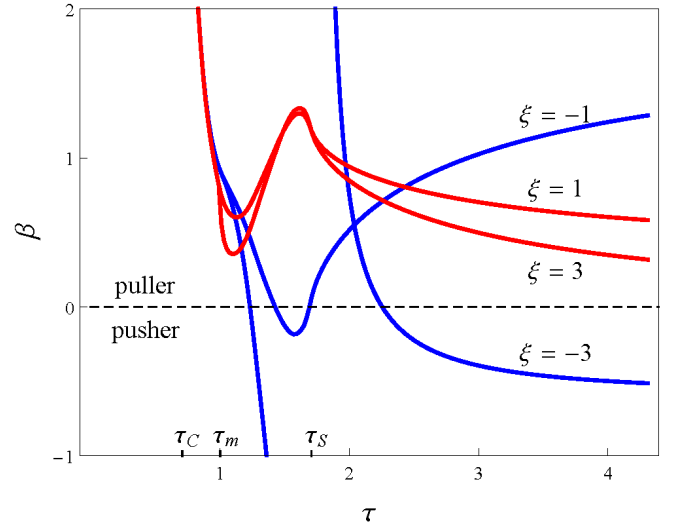


FIG. 4: Squirmer parameter  $\beta$ . For  $\tau \rightarrow \tau_C$ , the active area reduces to a small spot, resulting in  $\beta = 5$  [24]. The divergence for  $\xi = -3$  occurs where the velocity  $v_P$  is zero.

[20]), measured for beads of different radius ( $a = 0.5\mu\text{m}$  and  $2.13\mu\text{m}$ ) in the range  $\tau \leq 1$  [24]. A strong discrepancy occurs for particles with hydrophilic caps, which move the cap at the rear, at both weak [4] and strong driving [20].

Some aspects of Fig. 3 disagree with a very recent theory paper [30]. As two main differences we note that Ref. [30] (i) assumes an isothermal cap with zero slip velocity and (ii) considers quite large velocities  $v_P > 10\mu\text{m/s}$ , where the water-lutidine kinetics is governed by advection rather than diffusion [24].

*Squirmer parameter* The interaction of a microswimmer with a wall and collective effects are to a large extent determined by the squirmer parameter  $\beta$  [10–12], which is defined through the even component of the slip velocity  $v_s = v_s^0 \sin \theta (1 + \beta \cos \theta)$  [31]. A “puller” is propelled by the activity of its front hemisphere ( $\beta > 0$ ), and a “pusher” by its back part ( $\beta < 0$ ).

In Fig. 4 we plot  $\beta$  as a function of  $\tau$  for different adsorption parameter ratios  $\xi$ . At the onset of self-propulsion, where the active area is reduced to a small spot at the summit of the cap, one finds

$$\beta = 5 \quad (\tau \rightarrow \tau_C). \quad (7)$$

(For a particle moving the active spot at the back, one has  $\beta = -5$ .) With increasing driving,  $\beta$  decreases rapidly and strongly depends on the reduced temperature  $\tau$  and the parameter  $\xi$ . Opposite affinities of the two hemispheres,  $\xi < 0$ , may result in pullers or pushers of variable strength; the singularity for  $\xi = -3$  occurs where the particle velocity changes sign. This means that a tiny change in the driving could significantly modify  $\beta$  and thus the collective behavior [10–12].

*Charge effects.* Surface charges have been shown to be relevant for the reversible aggregation of polystyrene par-

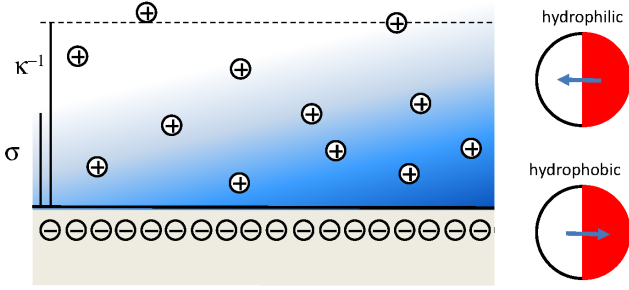


FIG. 5: Schematic view of the electric double layer with screening length  $\kappa^{-1}$ . The ions within the demixing volume of thickness  $\sigma$  diffuse toward higher water content. As a result, the particle moves backward (cap at the rear) for hydrophilic coating, and forward (cap at the front) for hydrophobic coating.

ticles in a near-critical water-lutidine mixture [32], and they may even change the sign of the critical Casimir effect [33]. Here we complete the above discussion of self-diffusiophoresis by including charge effects, as a possible explanation for the backward motion of beads with hydrophilic cap.

A composition gradient  $\nabla\phi$  along a charged surface gives rise to two distinct effects: the drift of the mobile counterions due to the ion-specific thermodynamic force  $-\nabla\mu$ , and the non-uniform properties of the electric double layer, very much like the thermal forces in a temperature gradient [28]. Here we discuss the ion-drift term only, and reduce the chemical potential to the electrostatic self-energy of a monovalent ion of radius  $a_m$ ,

$$\mu = \frac{e^2}{8\pi\epsilon a_m}. \quad (8)$$

The variation of the composition  $\phi$  in the demixing volume is illustrated in Fig. 5. The dependence of the permittivity  $\epsilon$  on  $\phi$  gives rise to a thermodynamic force density  $-\rho\partial_x\mu$  with the ion concentration  $\rho$ . This ion current drags the fluid along the particle surface and thus induces a slip velocity

$$v_s = -\frac{1}{\eta} \int_0^\infty dz z \rho \partial_x \mu. \quad (9)$$

Spelling out the gradient,  $\partial_x\mu = -\mu(\partial_\phi \ln \epsilon)\partial_x\phi$ , assuming the linear law  $\epsilon = \phi\epsilon_w + (1-\phi)\epsilon_l$  for the permittivity of water-lutidine, and using  $\epsilon_w \gg \epsilon_l$ , one finds  $\partial_x\mu = -\mu\partial_x\phi$ .

The particle velocity  $v_p$  is given by the surface average of the negative slip velocity. Evaluating the counterion concentration in Debye-Hückel approximation,  $\rho = (\epsilon/e)|\zeta|e^{-\kappa z}$ , we find [24]

$$v_p = -\frac{e|\zeta|}{8\pi\eta a_m} \int_{-1}^1 dc \frac{(1-c^2)\partial_c\phi}{[1+(\sigma\kappa)^{-1}]^2}, \quad (10)$$

which strongly depends on the ratio of the screening length  $\kappa^{-1}$  and the thickness  $\sigma$  of the demixing volume.

With typical parameters the prefactor takes a value of millimeters per second. Taking  $\sigma\kappa \sim \frac{1}{10}$  and  $\partial_c\phi \sim 0.1$  as suggested by Figs. 1 and 2, we find  $v_p \sim \mu\text{m/s}$ , which corresponds to measured values. So far we have considered the salt-free case where  $\kappa^{-1} \sim$  hundreds of nanometers. Adding salt would result in diffusiophoresis in a non-uniform electrolyte [34–36]. Moreover, we have discarded specific-ion effects which are not small in general [16, 37].

According to (10), charged particles move in the direction opposite to the composition gradient, that is, cap at the rear for water-adsorbing (hydrophilic) coating. This is precisely what was observed in experiments on particles with hydrophilic gold caps [4, 20]. The ionic end-groups used in these studies (11-mercaptopentadecanoic acid) cause a  $\zeta$ -potential of about  $-50$  mV [38], which results in a negative velocity  $v_p$  of microns per second.

On the other hand, the cap-at-the-front orientation, expected for lutidine-adsorbing (hydrophobic) charged surfaces, is probably of little relevance: The carbon caps [9] and hydrophobic gold caps (functionalized with 1-octadecanethiol) [20] carry only weak charges; as a consequence, their forward motion is due to the dispersion forces underlying (5).

*Conclusion.* Hot Janus particles in a near-critical water-lutidine mixture move due to their self-generated composition gradient. Our analysis reveals two main mechanisms: The dispersion forces exerted on water and lutidine result in a positive velocity  $v_p > 0$ , whereas at a charged surface, the counterions migrate toward higher water content and thus drive hydrophilic particles backward,  $v_p < 0$ . The first effect accounts for the observed forward motion of uncharged particles [9, 20], and the second one for the backward motion of beads with charged hydrophilic caps [4, 20].

Both the velocity  $v_p$  and the squirmer parameter  $\beta$  show a non-monotonous variation with the wetting properties and surface temperature; this implies that the hydrodynamic interactions related to  $\beta$  strongly depend on the driving power. The phase behavior of squirmer systems is very sensitive to the value of  $\beta$  [10–12]; in view of Fig. 4 it could be changed by tuning the heating.

As an outlook, our findings, both on the wetting properties and on charge effects, could be relevant for other driving mechanisms of active particles. Moreover, they suggest that the overlap of the critical droplets of nearby Janus particles should give rise to a complex interaction pattern, which could affect the observed aggregation behavior and result in a variety of reversible ordered states, similar to those realized recently with Janus particles in a homogenous near-critical water-lutidine mixture [23].

Helpful discussions with Y. Amarouchène, C. Bechinger, and U. Delabre are gratefully acknowledged. This work was supported by Agence Nationale de la Recherche through contract ANR-13-IS04-0003,

- 
- [1] W. F. Paxton, A. Sen, and T. E. Mallouk, *Chem. Eur. J.* **11**, 6462 (2005).
- [2] J.R. Howse, R.A.L. Jones, A.J. Ryan, T. Gough, R. Vafabakhsh, and R. Golestanian, *Phys. Rev. Lett.* **99**, 048102 (2007)
- [3] H.-R. Jiang, N. Yoshinaga, M. Sano, *Phys. Rev. Lett.* **105**, 268302 (2010)
- [4] G. Volpe, I. Buttinoni, D. Vogt, H.-J. Kümmerer, and C. Bechinger, *Soft Matter* **7**, 8810 (2011)
- [5] L. Baraban, R. Streubel, D. Makarov, L. Han, D. Karnausenko, O.G. Schmidt, G. Cuniberti, *ACS Nano* **7**, 1360 (2013)
- [6] B. Qian, D. Montiel, A. Bregulla, F. Cichos, H. Yang, *Chem. Sci.* **4**, 1420 (2013)
- [7] P.K. Ghosh, V.R. Misko, F. Marchesoni, F. Nori, *Phys. Rev. Lett.* **110**, 268301 (2013)
- [8] I. Theurkauff, C. Cottin-Bizonne, J. Palacci, C. Ybert, L. Bocquet, *Phys. Rev. Lett.* **108**, 268303 (2012)
- [9] I. Buttinoni, J. Bialké, F. Kümmel, H. Löwen, C. Bechinger, T. Speck, *Phys. Rev. Lett.* **110**, 238301 (2013)
- [10] T. Ishikawa, T. J. Pedley, *Phys. Rev. Lett.* **100**, 088103 (2008)
- [11] I. Llopis, I. Pagonabarraga, J. Non-Newtonian Fluid Mech. **165**, 946 (2010)
- [12] A. Zöttl, H. Stark, *Phys. Rev. Lett.* **112**, 118101 (2014)
- [13] S. Ebbens, J.R. Howse, *Soft Matter* **6**, 726 (2010)
- [14] R. Kapral, *J. Chem. Phys.* **138**, 020901 (2013)
- [15] J. Moran, P. Wheat, and J. Posner, *Phys. Rev. E* **81**, 065302 (2010).
- [16] A. Brown, W. Poon, *Soft Matter* **10**, 4016 (2014)
- [17] B.V. Derjaguin, G.P. Sidorenko, E.A. Zubashenko, E.B. Kiseleva, *Kolloid Zh.* **9**, 335 (1947).
- [18] N.V. Churaev, B.V. Derjaguin, V.M. Muller, *Surface Forces*, Plenum Publishing Corporation (New York 1987)
- [19] J. de Graaf, G. Rempfer, C. Holm, arXiv:1412.5331v1 (2014)
- [20] I. Buttinoni, G. Volpe, F. Kümmel, G. Volpe, C. Bechinger, *J. Phys.: Cond. Mat.* **24**, 284129 (2012)
- [21] T. Bickel, A. Majee, A. Würger, *Phys. Rev. E* **88**, 012301 (2013)
- [22] C.A. Grattoni, R.A. Dawe, C. Yen Seah, J.D. Gray, *J. Chem. Eng. Data* **38**, 516 (1993)
- [23] C. Yu, J. Zhang, S. Granick, *Angew.Chem. Int. Ed.* **53**, 1 (2014)
- [24] See the Supplementary Material [url], which includes Refs. [25–27]
- [25] S.R. de Groot, P. Mazur, *Non-equilibrium Thermodynamics*, North Holland Publishing, Amsterdam (1962)
- [26] J.C.R. Reis, T.P. Iglesias, G. Douhéret, M.I. Davis, *Phys.Chem.Chem.Phys.* **11**, 3977 (2009)
- [27] J.N. Agar, C.Y. Mou, J. Lin J, *J. Phys. Chem.* **93**, 2079 (1989)
- [28] A. Würger, *Rep. Prog. Phys.* **73**, 126601 (2010)
- [29] J.L. Anderson, *Ann. Rev. Fluid Mech.* **21**, 61 (1989)
- [30] S. Samin, R. van Roij, arXiv:1506.05695v1 (2015)
- [31] J.R. Blake, *J. Fluid Mech.* **46**, 199 (1971)
- [32] P.D. Gallagher, M.L. Kurnaz, J.V. Maher, *Phys. Rev. A* **46**, 7750 (1992)
- [33] A. Gambassi, A. Maciołek, C. Hertlein, U. Nellen, L. Helden, C. Bechinger, S. Dietrich, *Phys. Rev. E* **80**, 061143 (2009)
- [34] J.P. Ebel, J.L. Anderson, D.C. Prieve, *Langmuir* **4**, 396 (1988)
- [35] K.A. Eslahian, A. Majee, M. Maskos, A. Würger, *Soft Matter* **10**, 1931 (2014)
- [36] B. Abécassis et al., *Nature Mater.* **7**, 785 (2008)
- [37] R. Wang, Z.-G. Wang, *Phys. Rev. Lett.* **112**, 136101 (2014)
- [38] T. Laaksonen, P. Ahonen, C. Johans, K. Kontturi, *ChemPhysChem* **7**, 2143 (2006)